



A critical role for microglia in maintaining vascular integrity in the hypoxic spinal cord

Sebok K. Halder^a and Richard Milner^{a,1,2}

^aDepartment of Molecular Medicine, The Scripps Research Institute, La Jolla, CA 92037

Edited by Lawrence Steinman, Stanford University School of Medicine, Stanford, CA, and approved November 5, 2019 (received for review July 15, 2019)

Hypoxic preconditioning reduces disease severity in a mouse model of multiple sclerosis (MS), in part by enhancing the barrier properties of spinal cord blood vessels. Because other studies have shown that similar levels of hypoxia transiently increase permeability of central nervous system (CNS) blood vessels, the goal of this study was to define the impact of chronic mild hypoxia (CMH, 8% O₂) on the integrity of spinal cord blood vessels and the responses of neighboring glial cells. Using extravascular fibrinogen as a marker of vascular disruption, we found that CMH triggered transient vascular leak in spinal cord blood vessels, particularly in white matter, which was associated with clustering and activation of Mac-1-positive microglia around disrupted vessels. Microglial depletion with the colony stimulating factor-1 receptor (CSF-1R) inhibitor PLX5622, while having no effect under normoxic conditions, profoundly increased vascular leak in both white and gray matter during CMH, and this was associated with disruption of astrocyte-vascular coupling and enhanced loss of tight junction proteins. Microglial repair of leaky blood vessels was blocked by a peptide that inhibits the interaction between fibrinogen and its Mac-1 integrin receptor. These findings highlight an important role for microglia in maintaining vascular integrity in the hypoxic spinal cord and suggest that a fibrinogen-Mac-1 interaction underpins this response. As relative hypoxia is experienced in many situations including high altitude, lung disease, obstructive sleep apnea, and age-related CNS ischemia/hypoxia, our findings have important implications regarding the critical role of microglia in maintaining vascular integrity in the CNS.

spinal cord | blood vessels | microglia | hypoxia | fibrinogen

Central nervous system (CNS) blood vessels are unique in forming a tight barrier between the blood and parenchymal tissue, termed the blood-brain barrier (BBB). This confers high electrical resistance and low permeability properties, thus protecting neural cells from potentially harmful blood components (1–3). The molecular basis of the BBB depends on interendothelial tight junction proteins, the vascular basal lamina comprising extracellular matrix (ECM) proteins, and the influence of astrocyte end-feet and pericytes (4–7). BBB disruption occurs in a number of different neurological conditions, including ischemic stroke, multiple sclerosis (MS), meningitis, and CNS tumors (8–12), and there is evidence that BBB integrity deteriorates with aging (13, 14). Thus, from a therapeutic perspective, there is a high priority to define and fully understand the mechanisms that enhance BBB integrity as well as those that promote repair of previously disrupted CNS blood vessels.

While the severe hypoxia of ischemic stroke leads to widespread BBB disruption, paradoxically, a milder hypoxic insult induces beneficial adaptations in CNS blood vessels that protect against future ischemic insult (15, 16). Similarly, recent studies have shown that beneficial changes in spinal cord blood vessels may underpin the protective effect of chronic mild hypoxia (CMH, typically 8–10% O₂) in reducing clinical severity in the MS mouse model, experimental autoimmune encephalomyelitis (EAE) (17, 18). CMH triggers a strong vascular remodeling response throughout the brain and spinal cord, culminating in greater than 50% increased vessel density over a 2-wk period (19,

20). At the same time, endothelial expression of tight junction proteins is strongly up-regulated, suggesting enhanced vascular integrity (21, 22). However, several studies have demonstrated that mild hypoxia leads to transient and reversible reductions in BBB integrity in cerebral vessels (23, 24). As these processes have never been examined in spinal cord blood vessels and because of the relevance of this to MS/EAE pathogenesis, the central goal of this project was to determine how mild hypoxia influences vascular integrity in spinal cord blood vessels.

While the importance of endothelial cells, pericytes, and astrocytes in regulating vascular stability and remodeling is well established (1, 2, 4, 7, 25, 26), few studies have addressed the role of microglia in this process. This is relevant because microglia are the rapid reaction force that are always on surveillance, scanning the CNS for foreign antigens or incoming pathogens and launch a vigorous immune-mediated and phagocytic response when required (27). However, microglia represent a double-edged sword in that while they are initially protective, if they become chronically stimulated, they adopt a highly activated destructive phenotype that secrete proinflammatory cytokines as well as a variety of proteases that digest tissue (28). In light of the protective influence of hypoxic preconditioning in an animal model of MS (17, 18), the goal of this study was to examine the impact of CMH on spinal cord blood vessels with 3 specific questions in mind: First, how is vascular integrity altered during hypoxic-induced vascular remodeling; second, how do astrocytes and microglia respond during this remodeling process; and third, what is the contribution of microglia in regulating vascular integrity during hypoxic exposure?

Significance

We show that chronic mild hypoxia (CMH; 8% O₂) induces transient vascular leak in spinal cord blood vessels that is associated with microglial clustering. Microglial depletion profoundly increased vascular leak during CMH, and this was associated with astrocyte-vascular uncoupling and loss of tight junction proteins. Microglial repair of blood vessels was blocked by a peptide that inhibits fibrinogen-Mac-1 interactions. These findings highlight a critical role for microglia in maintaining vascular integrity in the hypoxic spinal cord and suggest that a fibrinogen-Mac-1 interaction underpins this response. As relative hypoxia is experienced during lung disease, sleep apnea, and age-related central nervous system (CNS) ischemia, our findings have important implications regarding the critical role of microglia in maintaining CNS vascular integrity.

Author contributions: R.M. designed research; S.K.H. performed research; S.K.H. and R.M. analyzed data; and R.M. wrote the paper.

The authors declare no competing interest.

This article is a PNAS Direct Submission.

Published under the PNAS license.

¹To whom correspondence may be addressed. Email: rmliner@sdbri.org.

²Present address: San Diego Biomedical Research Institute, San Diego, CA 92121.

This article contains supporting information online at <https://www.pnas.org/lookup/suppl/doi:10.1073/pnas.1912178116/-DCSupplemental>.

First published November 26, 2019.

Results

Mild Hypoxic Stress Triggers Transient Vascular Leak in Spinal Cord Blood Vessels That Is Associated with Microglial Clustering. The impact of CMH (8% O₂) on spinal cord vascular integrity was examined by dual-immunofluorescence (dual-IF) using CD31 to label endothelial cells and fibrinogen (Fbg) to detect extravascular leak. While no vascular leak was observed during normoxic conditions, CMH induced notable extravascular leak in a small number (~2–5%) of spinal cord blood vessels (Fig. 1A). Of note, these leaky blood vessels were observed predominantly in the white matter and rarely in gray matter. Analysis revealed that the number of leaky vessels/field of view (FOV) was highest during the active phase of vascular remodeling but declined at later time-points consistent with our finding that at this later time, blood vessels have largely completed their angiogenic remodeling response and stabilized (22, 29). Interestingly, dual-IF with fibrinogen and the microglial marker Mac-1 (CD11b/CD18) integrin revealed that extravascular fibrinogen leak was strongly associated with accumulation of microglial clustering around leaky blood vessels, and these microglia showed increased levels of the activation marker Mac-1 (Fig. 1C–E). As the studies presented in Fig. 1 were performed exclusively in female mice, we also examined this phenomenon in male mice and observed very similar results (*SI Appendix*, Fig. S1). Characterization of microglial activity by morphological criteria showed that in normoxic conditions or in fibrinogen-free areas (intact vessels) in CMH conditions, microglia displayed a ramified morphology (Fig. 1F). In contrast, most microglia associated with extravascular fibrinogen leak in CMH conditions displayed the classical activated morphology, with large cell body and short process extensions (Fig. 1F and G). To confirm that the Mac-1⁺ cells we observe clustering around leaking blood vessels are microglia and not blood-derived monocytes, we also labeled spinal cord sections with the microglia-specific marker Tmem119 (30), and this confirmed that the hypertrophic cells clustered around leaky blood vessels are microglia (*SI Appendix*, Fig. S2).

Microglial Depletion Leads to Exaggerated Vascular Leak during Mild Hypoxic Stress. To examine whether microglia play a vasculo-protective role during hypoxic exposure, we used a well-established pharmacological approach of depleting microglia by feeding mice with chow containing PLX5622, an inhibitor of colony stimulating factor 1 receptor (CSF-1R) (31). To confirm the efficacy of this approach, mice treated with 1200 ppm (1,200 mg of drug per kg of chow) PLX5622 for 7 d showed dramatically reduced numbers of microglia in spinal cord sections ($P < 0.01$; Fig. 2A and B). Consistent with previous reports, this treatment and the resulting microglial depletion had no apparent effect on the overall health of animals during this timeframe (31, 32).

Next, we pretreated mice with PLX5622 for 7 d, and while maintaining them on the PLX5622 diet, exposed them to CMH for periods of up to 14 d. Importantly, PLX5622-fed mice maintained under normoxic conditions showed no leaky vessels (*SI Appendix*, Fig. S3). However, after 7 d of hypoxia, while mice fed control chow contained just 1 or 2 leaky bloody vessels per spinal cord section, PLX5622-fed mice showed much greater numbers of leaky blood vessels at all time-points (Fig. 2C–E). Of note, while leaky blood vessels in control chow mice were located only in white matter, PLX5622-fed mice displayed leaky blood vessels throughout the white and gray matter (Fig. 2D). CD31/Fbg/Mac-1 triple-IF of the control chow mice confirmed microglial clustering and elevated levels of Mac-1 expression by microglia surrounding leaked fibrinogen, but as predicted, a total lack of microglial clustering in PLX5622-fed mice (Fig. 2F).

Under Hypoxic Conditions, Absence of Microglia Disrupts Astrocyte-Vascular Coupling, Leading to Increased MECA-32 Expression, a Marker of Leaky CNS Endothelium. Aquaporin-4 (AQP4) is a water channel protein expressed by astrocyte endfeet that plays an important role

in regulating vascular integrity in the CNS and is often used as an indicator of astrocyte-vascular coupling (33). As microglial depletion results in greater vascular leak in the spinal cord of mice exposed to CMH, we investigated whether absence of microglia impacts astrocyte-vascular coupling by performing CD31/AQP4 dual-IF on spinal cord sections from mice exposed to normoxic or hypoxic conditions in the absence or presence of PLX5622 (Fig. 3A and B). In the normoxic spinal cord, all blood vessels were AQP4-positive and absence of microglia had no impact on the number of AQP4-positive blood vessels (Fig. 3B). However, after 7 d of hypoxia, while almost all blood vessels in normal chow-fed mice were AQP4-positive, a significant number of vessels in PLX5622-fed mice lacked AQP4 expression ($P < 0.01$). High magnification CD31/IgG/AQP4 triple-IF images (Fig. 3E) demonstrated that under hypoxic conditions, almost all spinal cord blood vessels in normal chow-fed mice expressed AQP4 and showed no extravascular IgG leak. In contrast, PLX5622-fed mice showed extravascular IgG leak that was strongly associated with disruption of vascular AQP4 expression. Additional CD31/Mac-1/AQP4 triple-IF images showed that under normoxic conditions, Mac-1⁺ microglia make discrete point contacts with several different blood vessels, but when surrounding a leaky blood vessel under hypoxic conditions, microglia surround and envelop the leaky blood vessel (*SI Appendix*, Fig. S4). In an alternative approach to examine whether microglial ablation impacts vascular integrity in CMH-treated mice, we analyzed MECA-32 expression, a marker of CNS blood vessels with compromised vascular integrity (34, 35). No MECA-32 expression was detected under normoxic conditions, either in control or PLX5622-fed mice (*SI Appendix*, Fig. S5). However, in mice exposed to CMH, PLX5622-fed mice showed a greatly increased number of MECA-32-positive vessels compared to normal chow fed mice at all time-points ($P < 0.05$) (Fig. 3C). These findings confirm that in mice exposed to CMH, absence of microglia leads to astrocyte-vascular uncoupling and reduced vascular integrity.

Microglial Depletion Also Results in Loss of Endothelial Tight Junction Protein Expression in Mice Exposed to CMH. As endothelial tight junction proteins are a key component of vascular integrity (1–3), we next examined how microglial depletion affects tight junction protein expression on spinal cord blood vessels following CMH (Fig. 4A and C). In keeping with previous findings (21, 22), quantification of total fluorescent signal revealed that in mice fed normal chow, CMH enhanced vascular expression of the tight junction proteins occludin and ZO-1 (Fig. 4B and D). However, at all timepoints examined, PLX5622-fed mice showed reduced expression of ZO-1 and occludin compared with mice fed normal chow. This is well illustrated at the 7-d timepoint in Fig. 4A and C, which reveals a significant number of vessels in PLX5622-fed mice lacking ZO-1 or occludin expression (denoted by arrows). High magnification triple-IF images with CD31/IgG/ZO-1 or CD31/IgG/occludin showed that in mice fed normal chow, blood vessels expressed high levels of ZO-1 and occludin, correlating with no IgG extravascular leak (Fig. 4E and F, respectively). In contrast, PLX5622-treated mice showed extravascular IgG leak that was strongly associated with disruption or absence of endothelial ZO-1 and occludin expression. These data support the idea that microglial absence leads to greater vascular disruption underpinned by loss of endothelial tight junction protein expression.

Microglial Repair of Leaky Blood Vessels Is Blocked by a Fibrinogen-Derived Inhibitory Peptide. In light of previous studies that the interaction between extravascular fibrinogen and the microglial cell surface receptor Mac-1 integrin promotes microglial clustering around leaky blood vessels in an EAE model of MS (36), we wondered if the same mechanism might mediate vascular repair during hypoxia-associated vascular disruption. To test this

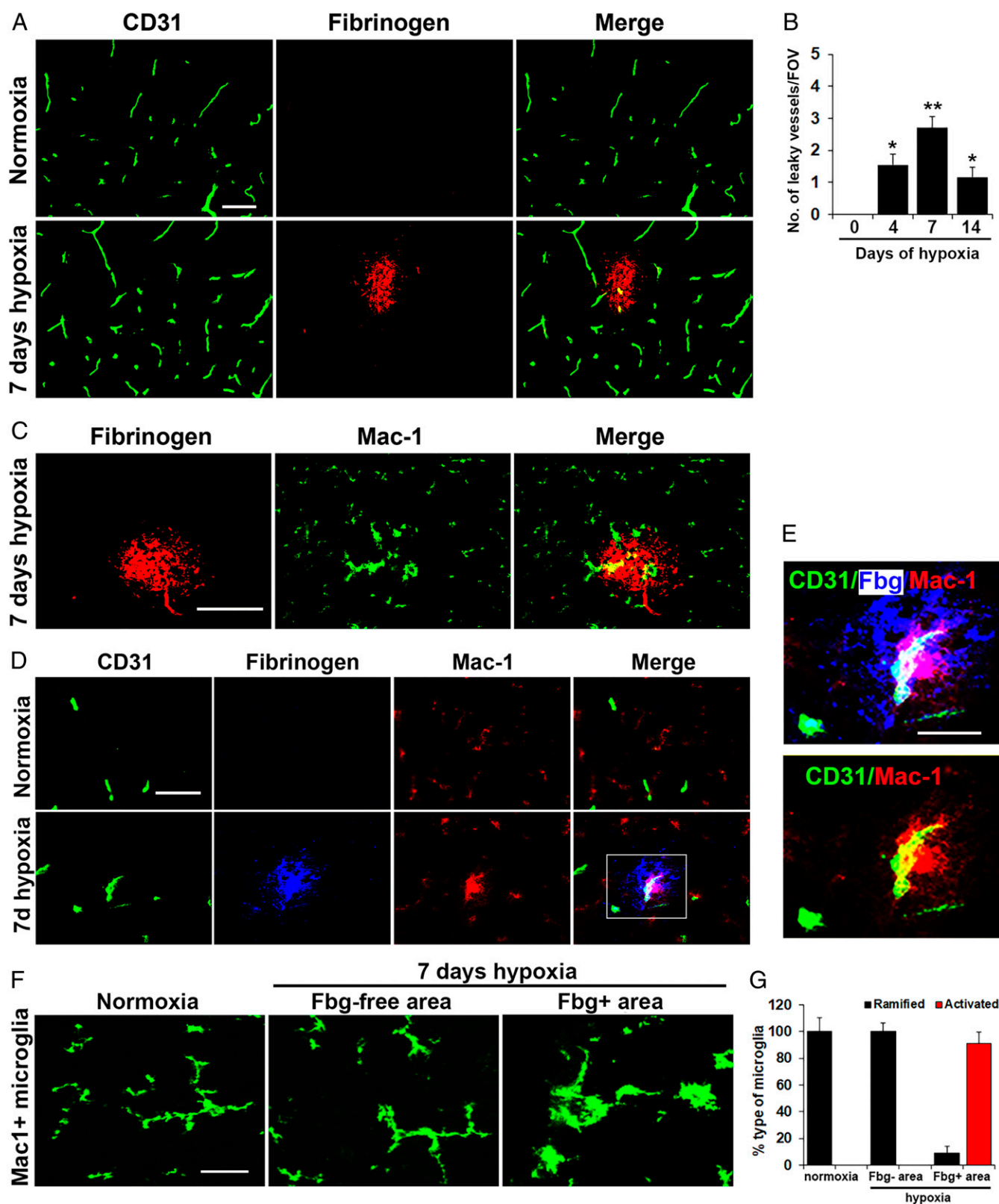


Fig. 1. Mild hypoxic stress triggers vascular leak in spinal cord blood vessels associated with microglial clustering. Frozen sections of lumbar spinal cord taken from mice exposed to normoxia or 7-d hypoxia (8% O₂) were stained for the following markers: the endothelial marker CD31 (Alexa Fluor 488) and fibrinogen (Cy-3) (A); fibrinogen (Cy-3) and Mac-1 (Alexa Fluor 488) (C); CD31 (Alexa Fluor 488), fibrinogen (abbreviated to Fbg in E) Cy-5 (blue) and Mac-1 (Cy-3) (D and E); and Mac-1 (Alexa Fluor 488) (F). (B) Quantification of the number of leaky (fibrinogen-positive) vessels/FOV. (G) Quantification of the morphological categorization of microglia under different conditions. Results are expressed as the mean ± SEM (*n* = 6 mice per group). **P* < 0.05, ***P* < 0.01 vs. normoxic conditions. One-way ANOVA followed by Tukey's multiple comparison test. Note that CMH induced transient vascular leak in spinal cord blood vessels that was associated with wrapping of Mac-1-positive microglial processes around the damaged vessel (high power images in E) and with morphological switch from ramified to activated morphology (F). (Scale bars, 50 μm; except for E, 25 μm.)

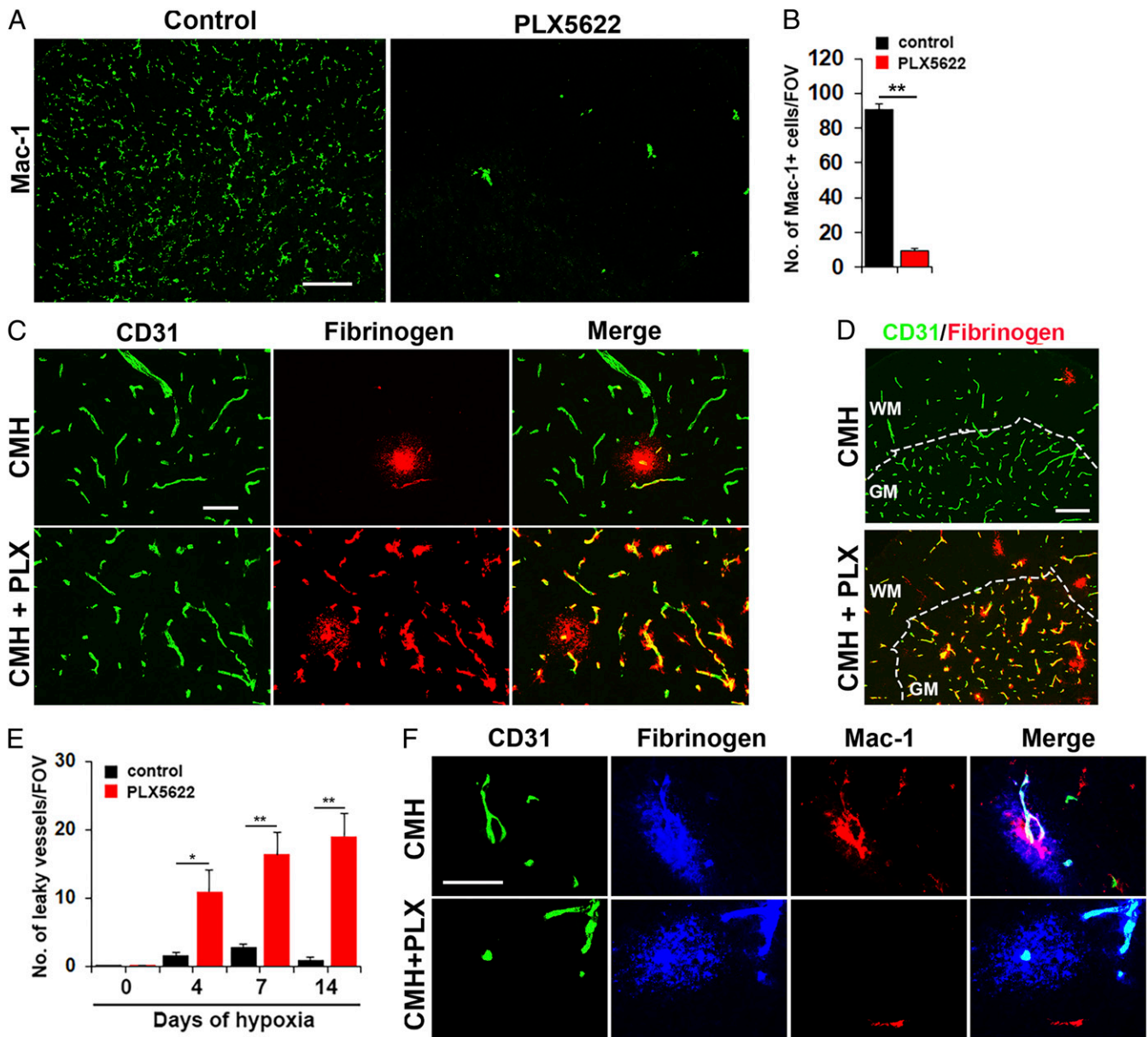


Fig. 2. Microglial depletion results in exaggerated vascular leak during CMH. (A) Frozen sections of lumbar spinal cord taken from mice fed normal chow or PLX5622-containing chow and maintained under normoxic conditions for 7 d were stained for the microglial marker Mac-1. (B) Quantification of microglial depletion after 7-d PLX5622. Results are expressed as the mean \pm SEM ($n = 6$ mice per group). Note that 7-d PLX5622 reduced the number of spinal cord microglia to 10% of untreated controls. (C and D) Frozen sections of lumbar spinal cord taken from mice fed normal chow or PLX5622-containing chow and maintained under hypoxic conditions for 7 d were stained for CD31 (Alexa Fluor 488) and fibrinogen (Cy-3). (E) Quantification of the number of leaky vessels/FOV. Results are expressed as the mean \pm SEM ($n = 6$ mice per group). * $P < 0.05$, ** $P < 0.01$. One-way ANOVA followed by Tukey's multiple comparison test. Note that PLX5622-treated mice showed a much greater number of leaky blood vessels. (F) CD31/fibrinogen/Mac-1 triple-IF of control chow mice confirmed microglial clustering and elevated levels of Mac-1 expression by microglia surrounding the leaky vessel, but absence of microglial clustering in PLX5622-fed mice. (Scale bars, A, 100 μm ; C, 50 μm ; D, 100 μm ; F, 25 μm .)

idea, we exposed mice to hypoxia for periods of up to 7 d, while at the same time treating them with daily intraperitoneal (i.p.) injections of the fibrinogen-derived inhibitory peptide $\gamma^{377-395}$ that blocks the interaction of fibrinogen with its Mac-1 integrin receptor, and then after 4 or 7 d CMH, quantified the number of leaky blood vessels in spinal cord sections. This showed that spinal cords of mice receiving the inhibitory $\gamma^{377-395}$ peptide contained significantly higher numbers of leaky blood vessels compared to control mice that received a scrambled peptide at all timepoints (Fig. 5A and B). In addition, the $\gamma^{377-395}$ inhibitory peptide prevented the migration and accumulation of activated microglia around leaky blood vessels

(Fig. 5C). These findings demonstrate that microglial recruitment and repair of leaking blood vessels is dependent on a fibrinogen-Mac-1-mediated mechanism.

Discussion

Our studies highlight an important role for microglia in maintaining vascular integrity in the hypoxic spinal cord and suggest that a fibrinogen-Mac-1 interaction underpins this response. We demonstrate that in the mouse spinal cord, CMH results in a transient vascular leak in a small minority of blood vessels, primarily in white matter, an effect that peaks within the first 7 d of

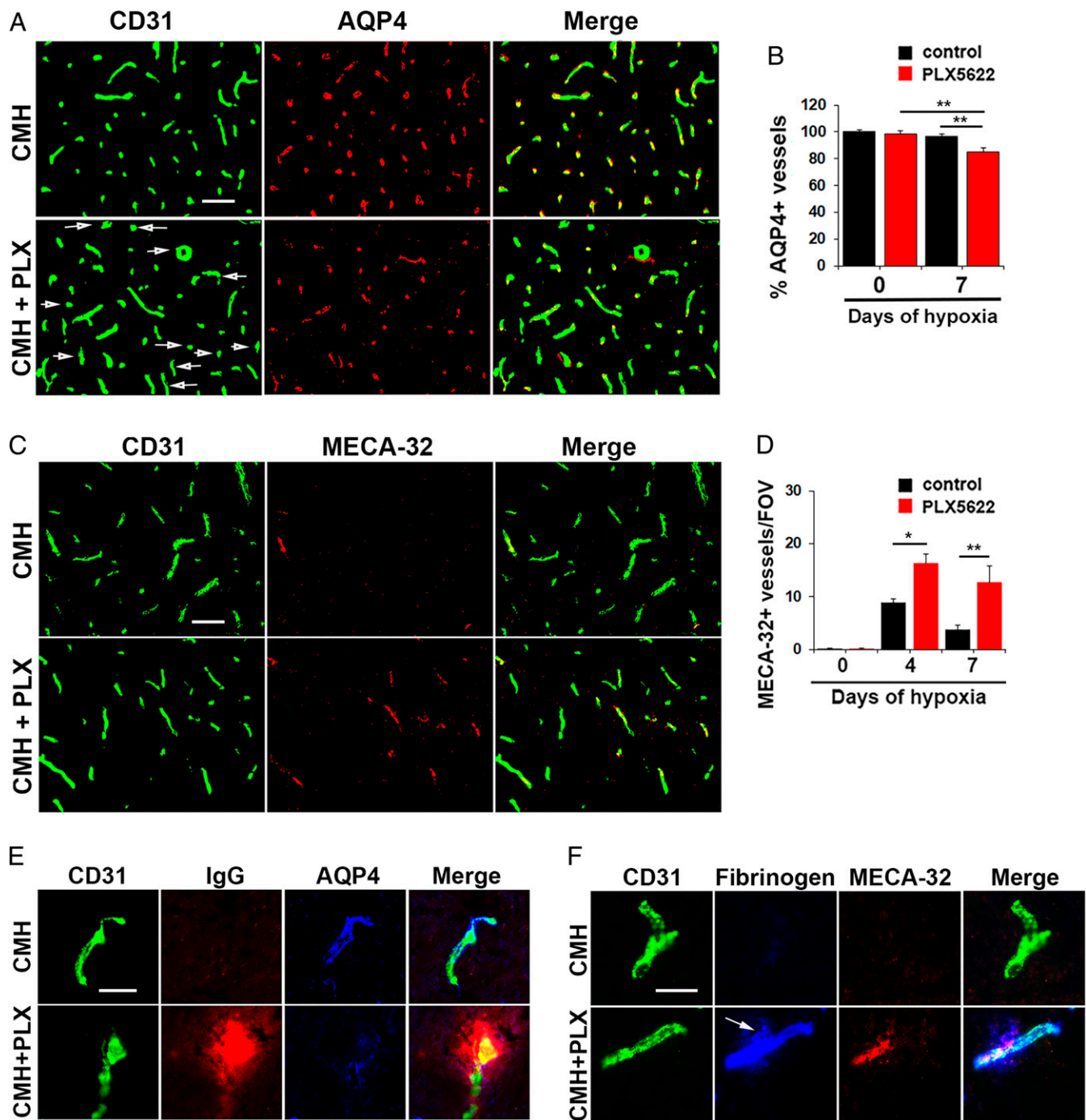


Fig. 3. Under hypoxic conditions, absence of microglia disrupts astrocyte-vascular coupling, leading to increased MECA-32 expression. (A and C) Frozen sections of lumbar spinal cord taken from mice fed normal chow or PLX5622-containing chow and maintained under hypoxic conditions for 7 d were stained for CD31 (Alexa Fluor 488) and AQP4 (Cy-3) in A or CD31 (Alexa Fluor 488) and MECA-32 (Cy-3) in C. (B and D) Quantification of the percent of blood vessels expressing AQP4 (B) or number of blood vessels expressing MECA-32/FOV (D). Results are expressed as the mean \pm SEM ($n = 6$ mice per group). * $P < 0.05$, ** $P < 0.01$. One-way ANOVA followed by Tukey's multiple comparison test. Note that under hypoxic conditions, spinal cords of PLX5622-fed mice contained a significant number of blood vessels that lacked AQP4 expression (see arrows) and showed greater induction of MECA-32. (E and F) High-magnification CD31/IgG/AQP4 or CD31/fibrinogen/MECA-32 triple-IF images show that under hypoxic conditions, spinal cord blood vessels in PLX5622-treated mice showed increased extravascular leak that was strongly associated with loss of AQP4 and induction of MECA-32 expression (see arrow). (Scale bars, A and C, 50 μ m; E and F, 25 μ m.)

CMH exposure, and then recedes. The timing of this vascular leak correlates closely with the vascular remodeling events induced by CMH whereby endothelial cells uncouple from their neighbors and migrate to extend new sprouts (22, 29). How can an initial vascular leak translate into a longer-term beneficial effect that actually enhances vascular integrity? Our data support

the notion that the initial leak is only transient but then stimulates adaptive responses within blood vessels that lead to enhancement of vascular integrity, including up-regulated endothelial expression of tight junction proteins and expression of ECM proteins such as laminin in the vascular basement membrane (18, 21, 22). It was notable that in mice with normal microglial levels, vascular leak in

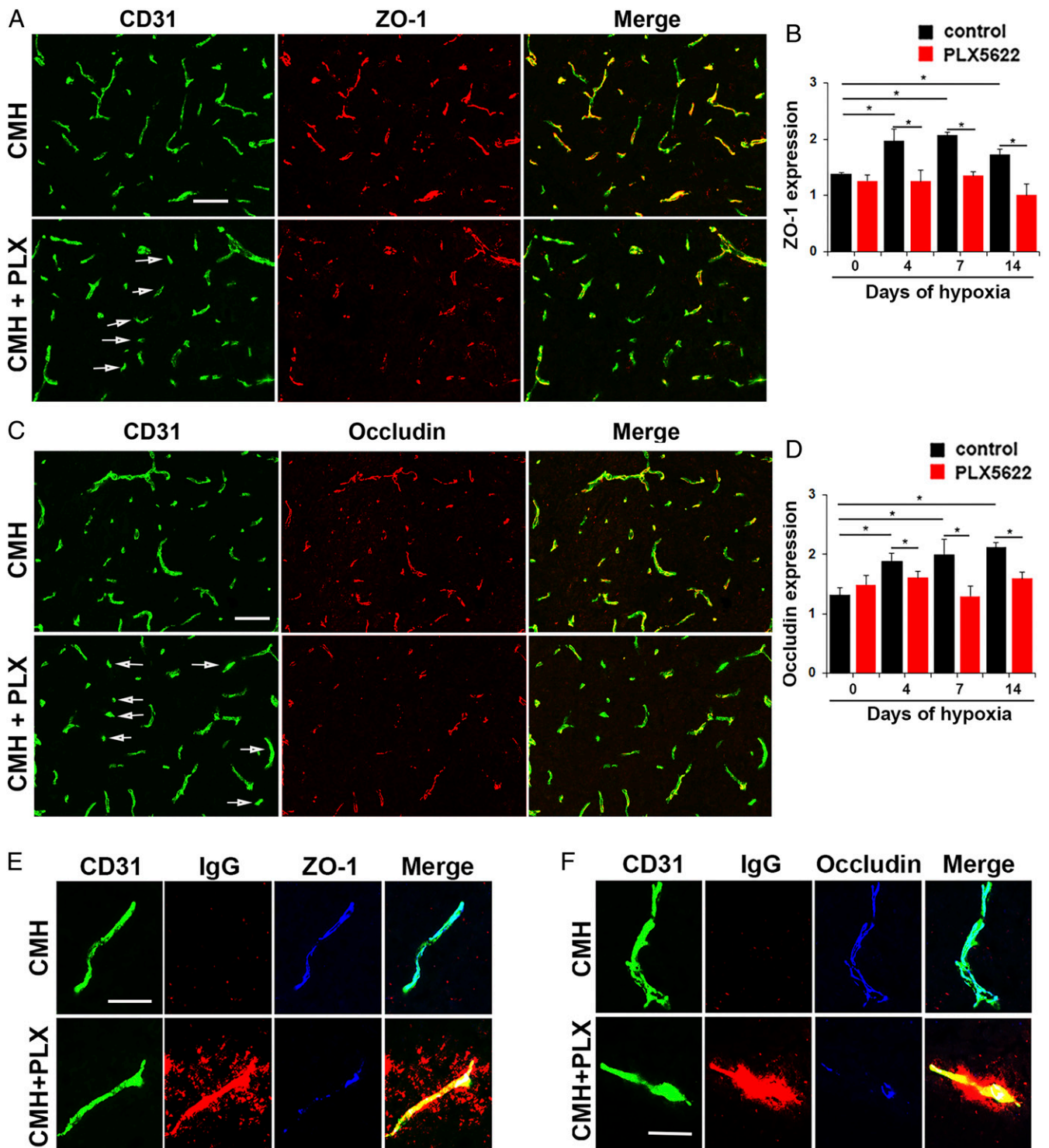


Fig. 4. Microglial depletion results in loss of endothelial tight junction protein expression during CMH. (A and C) Frozen sections of lumbar spinal cord taken from mice fed normal chow or PLX5622-containing chow and maintained under hypoxic conditions for 7 d were stained for CD31 (Alexa Fluor 488) and ZO-1 (Cy-3) in A or CD31 (Alexa Fluor 488) and occludin (Cy-3) in C. (B and D) Quantification of endothelial expression of ZO-1 (B) or occludin (D). Results are expressed as the mean \pm SEM ($n = 6$ mice per group). * $P < 0.05$. One-way ANOVA followed by Tukey's multiple comparison test. Note that under hypoxic conditions, spinal cords of PLX5622-fed mice showed focal areas in which blood vessels showed diminished expression of ZO-1 and occludin (see arrows in A and C). (E and F) High-magnification CD31/IgG/ZO-1 or CD31/IgG/occludin triple-IF images show that under hypoxic conditions, in mice fed normal chow, blood vessels expressed high levels of ZO-1 and occludin, correlating with no IgG extravascular leak, but in contrast, vessels in PLX5622-treated mice showed extravascular IgG leak that was strongly associated with disrupted endothelial ZO-1 and occludin expression. (Scale bars, A and C, 50 μ m; E and F, 25 μ m.)

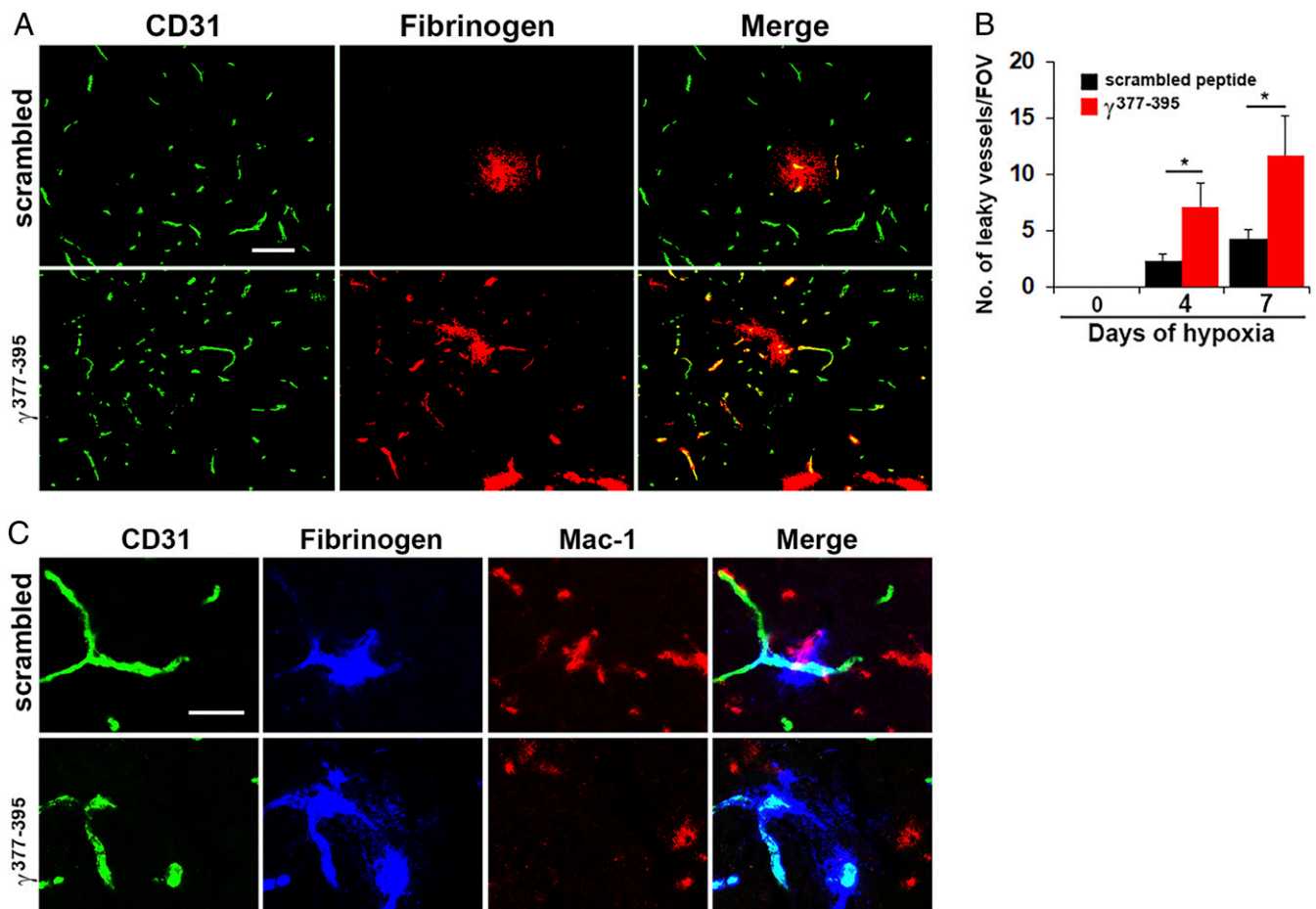


Fig. 5. Microglial vascular repair is blocked by a fibrinogen-derived inhibitory peptide. (A and C) Frozen sections of lumbar spinal cord taken from mice maintained under hypoxic conditions for 7 d that received daily injections of either the fibrinogen-derived inhibitory peptide $\gamma^{377-395}$ or a scrambled peptide, were stained for CD31 (Alexa Fluor 488) and fibrinogen (Cy-3) in A or CD31 (Alexa Fluor 488), fibrinogen (Cy-5, blue), and Mac-1 (Cy-3) in C. (B) Quantification of the number of leaky vessels/FOV. Results are expressed as the mean \pm SEM ($n = 6$ mice per group). * $P < 0.05$. One-way ANOVA followed by Tukey's multiple comparison test. Note that mice treated with the inhibitory peptide $\gamma^{377-395}$ showed a greater number of leaky blood vessels and the peptide prevented the migration and accumulation of activated microglia around leaky blood vessels (C). (Scale bars, A, 50 μm ; C, 25 μm .)

spinal cord vessels typically occurred only in white matter, so what accounts for this specificity? Most likely this is related to the fact that CMH induces a stronger vascular remodeling response in spinal cord white matter compared with gray matter, consistent with the idea that more vascular remodeling is associated with greater uncoupling of endothelial cells, leading to higher levels of vascular leak (21). Exactly why white matter is the site of greater vascular remodeling and vascular leak is still an open question, but this may be related to the low vascular density in white matter (approximately only 25% of that in gray matter) (37, 38), thus with a low functional reserve any drop in the rate of oxygen delivery has to be compensated by a stronger remodeling response in white matter.

Several studies have described microglial accumulation around disrupted CNS blood vessels, although in each study, different conclusions have been drawn. For instance, in the EAE mouse model of MS, the Akassoglou laboratory found that extravascular leak of fibrinogen attracted microglia to leaking blood vessels, concluding that fibrinogen stimulates microglia into an activated destructive phenotype, leading to demyelination (36). Our findings are similar in showing that microglial surround extravascular leaked fibrinogen and are dependent on the fibrinogen–Mac-1 integrin interaction, but whereas the former study proposed this as a pathological mechanism, our studies demonstrate that microglia play an important protective role in reducing vascular leak from spinal cord vessels under hypoxic conditions. Based on this, we

propose that the distinction between microglia playing a protective or pathogenic role could depend on the timing and/or severity of insult. In this model, during the early phase of vascular leak, microglia mediate a protective response to maintain vascular integrity, but in the face of continued vascular leak, microglia may become inappropriately stimulated into a phagocytic phenotype. This model would also explain the findings of Jolivel et al. (39) who showed that in the early stages of a mouse model of ischemic stroke, microglia congregate around damaged blood vessels, consistent with our findings, but in this severe model of ischemic/hypoxic insult, microglia eventually switch from a repair into a phagocytotic phenotype that remove the dying endothelial cells. The trigger that tips microglia from protective into phagocytic mode may be a function of time or degree of stimulation, perhaps mediated by the overall integral of incoming activation signals that microglia transduce, which would include signals from cytokines and chemokines as well as serum ECM proteins such as fibrinogen. Alternatively, another possibility is that the generation of oxygen free radicals that accompanies reperfusion following temporary ischemic stroke also plays a key role in triggering microglial switch into phagocytic mode. Our findings are also consistent with other reports in diabetic mouse and laser ablation models, demonstrating an important function for microglia in repairing damaged cerebral blood vessels (40, 41).

In these studies, we showed that CMH results in a transient vascular leak in a small minority of spinal cord blood vessels, an effect that peaks within the first 7 d of CMH exposure, and then recedes. As fibrinogen is a relatively large molecule (molecular mass ~340 kDa), this is most likely a relatively late indicator of vascular breakdown and only labels quite severe disruptions in vascular integrity. Therefore, in future studies we plan to use molecular probes of varying size (sodium fluorescein, FITC-dextran) to more closely characterize the time-course of this hypoxic-induced vascular leak. At the same time, we will also chart the dose–response of this vascular leak by exposing mice to different levels of hypoxia (from 8 to 16% O₂). Using this approach, we will also seek to understand whether the size of the leak equates to the efficacy or magnitude of the microglial repair response.

Unlike previous studies that examined microglial–vascular interactions in animal models of severe pathological disease involving extensive vascular damage (MS, stroke, diabetes mellitus) (36, 39, 41), our experiments were performed in a subclinical model of mild hypoxia (19, 20, 22). This is important because people experience relative hypoxia in a wide variety of situations, including visiting high altitude locations, lung disease (e.g., chronic obstructive pulmonary disease [COPD], obstructive sleep apnea, and experiencing age-related ischemia/hypoxia; refs. 13, 42, and 43), thus it seems likely that microglia are constantly monitoring and sealing these vascular leaks. From a clinical viewpoint, this has several implications. First, drugs that interfere with microglial function, e.g., minocycline, could suppress this protective effect and thereby predispose to worse vascular leak and CNS damage (44). Second, people with COPD or sleep apnea or those predisposed to ischemic stroke most likely suffer varying levels of intermittent hypoxia for months or years before any clinically detectable event. Based on our studies, it seems likely that microglia may be playing a vital role during this time by repairing hypoxic-induced vascular leaks as they occur. Third, during the process of aging, CNS vascular integrity is gradually diminished (13, 14), which raises the question: Is this a result of age-related vascular degeneration or is it due to reduced microglial repair function, and irrespective of the cause, could vascular integrity in the elderly be enhanced by promoting this protective microglial response? A greater understanding of these age-related events would facilitate improved design of therapeutic strategies aimed at influencing microglial function to optimize their vasculo-protective activity.

Materials and Methods

Animals. The studies described were reviewed and approved by The Scripps Research Institute (TSRI) Institutional Animal Care and Use Committee. WT female and male C57BL/6J mice obtained from the TSRI rodent breeding colony were maintained under pathogen-free conditions in the closed breeding colony of TSRI.

Chronic Hypoxia Model. Female or male WT C57BL/6J mice, 8–10 wk of age, were housed 4 to a cage, and placed into a hypoxic chamber (Biospherix) maintained at 8% O₂ for periods up to 14 d. Littermate control mice were kept in the same room under similar conditions except that they were kept at ambient sea-level oxygen levels (normoxia, ~21% O₂ at sea level) for the duration of the experiment. Every few days, the chamber was briefly opened for cage cleaning and food and water replacement as needed.

Elimination of Microglia. PLX5622 was provided by Plexxikon under Material Transfer Agreement and formulated in AIN-76A standard chow by Research Diets at a dose of 1,200 p.p.m. (1,200 mg of PLX5622 in 1 kg of chow). In microglial depletion experiments, mice were fed a PLX5622 diet for 7 d prior to them being placed in the hypoxic chamber to deplete microglia before mice were exposed to hypoxic conditions. Once in the hypoxic chamber, these mice were then maintained on the PLX5622 diet for the duration of the experiment (up to 14 d). Consistent with the findings of others, in these studies we found no obvious behavioral alterations, weight loss, or signs of illness in mice fed a PLX5622 diet for 3 wk (31, 32).

i.p. Administration of the Fibrinogen-Derived Inhibitory Peptide $\gamma^{377-395}$. The fibrinogen-derived inhibitory peptide $\gamma^{377-395}$ (YSMKETTMKIIPFNRLSIG) or the scrambled peptide (KMMISYTFPIERTGLISNK) previously described (36) were resuspended in phosphate buffer saline (PBS) at a concentration of 3 mg/mL and aliquoted as single doses and stored at –80 °C. At the same time mice were placed in the hypoxia chamber, they received daily i.p. injections containing 30 μ g of the fibrinogen-derived $\gamma^{377-395}$ inhibitory peptide or the scrambled control peptide. After 4 or 7 d of this treatment, mice were euthanized, and their spinal cord tissues were placed analyzed by immunohistochemistry for evidence of vascular breakdown.

Immunohistochemistry and Antibodies. Immunohistochemistry was performed on 10- μ m frozen sections of cold PBS perfused tissues as described previously (45). Rat monoclonal antibodies from BD Pharmingen reactive for the following antigens were used in this study: CD31 (clone MEC13.3), MECA-32, and Mac-1 (clone M1/70). The hamster anti-CD31 (clone 2H8) and rabbit anti-Tmem119 (clone 28-3) monoclonal antibodies were obtained from Abcam. Rabbit antibodies reactive for the following proteins were also used: occludin and ZO-1 (all from Invitrogen), fibrinogen (Millipore), and aquaporin-4 (AQP4) (Alomone Labs). Secondary antibodies used included Cy3-conjugated anti-rabbit, anti-rat, and anti-mouse and Cy5-conjugated anti-rabbit from Jackson ImmunoResearch and Alexa Fluor 488-conjugated anti-rat, anti-hamster, and anti-rabbit from Invitrogen.

Image Analysis. Images were taken using a 2 \times , 10 \times , or 20 \times objective on a Keyence 710 fluorescent microscope. All analysis was performed in the lumbar spinal cord. For each antigen in all analyses, images at least three randomly selected areas were taken at 10 \times or 20 \times magnification per tissue section and three sections per spinal cord analyzed to calculate the mean for each animal ($n = 6$ mice per group). For each antigen in each experiment, exposure time was set to convey the maximum amount of information without saturating the image and was maintained constant for each antigen across the different experimental groups. The number of leaking blood vessels was quantified by capturing images and performing manual counts of the number of vessels showing extravascular leaked fibrinogen. The number of microglia per FOV and the percentage or number of blood vessels expressing AQP4 or MECA-32 was quantified in a similar manner. Expression of the tight junction proteins ZO-1 and occludin was quantified by measuring the total fluorescent signal per FOV and analyzed using NIH ImageJ software. In the analysis of microglial activity by morphological criteria, the number of microglia displaying a ramified or activated (large cell body and short process extensions) phenotype in specific regions were quantified and expressed as a percentage. Each experiment was performed with 6 different animals per condition, and the results expressed as the mean \pm SEM. Statistical significance was assessed using one-way analysis of variance (ANOVA) followed by Tukey's multiple comparison post hoc test, in which $P < 0.05$ was defined as statistically significant.

Data Availability. The datasets used and/or analyzed during the current study are available from the corresponding author on reasonable request.

ACKNOWLEDGMENTS. This work was supported by NIH R56 Grant NS095753.

1. P. Ballabh, A. Braun, M. Nedergaard, The blood-brain barrier: An overview: Structure, regulation, and clinical implications. *Neurobiol. Dis.* **16**, 1–13 (2004).
2. J. D. Huber, R. D. Egleton, T. P. Davis, Molecular physiology and pathophysiology of tight junctions in the blood-brain barrier. *Trends Neurosci.* **24**, 719–725 (2001).
3. W. M. Pardridge, Blood-brain barrier drug targeting: The future of brain drug development. *Mol. Interv.* **3**, 90–105 (2003).
4. R. Daneman, L. Zhou, A. A. Kebede, B. A. Barres, Pericytes are required for blood-brain barrier integrity during embryogenesis. *Nature* **468**, 562–566 (2010).
5. G. J. del Zoppo, R. Milner, Integrin-matrix interactions in the cerebral microvasculature. *Arterioscler. Thromb. Vasc. Biol.* **26**, 1966–1975 (2006).
6. T. Osada *et al.*, Interendothelial claudin-5 expression depends on cerebral endothelial cell-matrix adhesion by $\beta(1)$ -integrins. *J. Cereb. Blood Flow Metab.* **31**, 1972–1985 (2011).
7. H. Wolburg, A. Lippoldt, Tight junctions of the blood-brain barrier: Development, composition and regulation. *Vascul. Pharmacol.* **38**, 323–337 (2002).
8. J. Bennett *et al.*, Blood-brain barrier disruption and enhanced vascular permeability in the multiple sclerosis model EAE. *J. Neuroimmunol.* **229**, 180–191 (2010).
9. D. C. Davies, Blood-brain barrier breakdown in septic encephalopathy and brain tumours. *J. Anat.* **200**, 639–646 (2002).
10. D. Gay, M. Esiri, Blood-brain barrier damage in acute multiple sclerosis plaques. An immunocytological study. *Brain* **114**, 557–572 (1991).

11. J. Kirk, J. Plumb, M. Mirakhor, S. McQuaid, Tight junctional abnormality in multiple sclerosis white matter affects all calibres of vessel and is associated with blood-brain barrier leakage and active demyelination. *J. Pathol.* **201**, 319–327 (2003).
12. J. Roberts, L. de Hoog, G. J. Bix, Mice deficient in endothelial $\alpha 5$ integrin are profoundly resistant to experimental ischemic stroke. *J. Cereb. Blood Flow Metab.* **37**, 85–96 (2017).
13. W. R. Brown, C. R. Thore, Review: Cerebral microvascular pathology in ageing and neurodegeneration. *Neuropathol. Appl. Neurobiol.* **37**, 56–74 (2011).
14. A. J. Farrall, J. M. Wardlaw, Blood-brain barrier: Ageing and microvascular disease—Systematic review and meta-analysis. *Neurobiol. Aging* **30**, 337–352 (2009).
15. J. Dowden, D. Corbett, Ischemic preconditioning in 18- to 20-month-old gerbils: Long-term survival with functional outcome measures. *Stroke* **30**, 1240–1246 (1999).
16. A. M. Stowe, T. Altay, A. B. Freie, J. M. Gidday, Repetitive hypoxia extends endogenous neurovascular protection for stroke. *Ann. Neurol.* **69**, 975–985 (2011).
17. P. Dore-Duffy, M. Wencel, V. Katyshev, K. Cleary, Chronic mild hypoxia ameliorates chronic inflammatory activity in myelin oligodendrocyte glycoprotein (MOG) peptide induced experimental autoimmune encephalomyelitis (EAE). *Adv. Exp. Med. Biol.* **701**, 165–173 (2011).
18. S. K. Halder, R. Kant, R. Milner, Hypoxic pre-conditioning suppresses experimental autoimmune encephalomyelitis by modifying multiple properties of blood vessels. *Acta Neuropathol. Commun.* **6**, 86 (2018).
19. J. C. LaManna, J. C. Chavez, P. Pichiule, Structural and functional adaptation to hypoxia in the rat brain. *J. Exp. Biol.* **207**, 3163–3169 (2004).
20. J. C. LaManna, L. M. Vendel, R. M. Farrell, Brain adaptation to chronic hypobaric hypoxia in rats. *J. Appl. Physiol.* **72**, 2238–2243 (1992).
21. S. K. Halder, R. Kant, R. Milner, Chronic mild hypoxia promotes profound vascular remodeling in spinal cord blood vessels, preferentially in white matter, via an $\alpha 5 \beta 1$ integrin-mediated mechanism. *Angiogenesis* **21**, 251–266 (2018).
22. L. Li *et al.*, In the hypoxic central nervous system, endothelial cell proliferation is followed by astrocyte activation, proliferation, and increased expression of the $\alpha 6 \beta 4$ integrin and dystroglycan. *Glia* **58**, 1157–1167 (2010).
23. A. T. Bauer, H. F. Bürgers, T. Rabie, H. H. Marti, Matrix metalloproteinase-9 mediates hypoxia-induced vascular leakage in the brain via tight junction rearrangement. *J. Cereb. Blood Flow Metab.* **30**, 837–848 (2010).
24. H. J. Schoch, S. Fischer, H. H. Marti, Hypoxia-induced vascular endothelial growth factor expression causes vascular leakage in the brain. *Brain* **125**, 2549–2557 (2002).
25. R. C. Janzer, M. C. Raff, Astrocytes induce blood-brain barrier properties in endothelial cells. *Nature* **325**, 253–257 (1987).
26. K. Wolburg-Buchholz *et al.*, Loss of astrocyte polarity marks blood-brain barrier impairment during experimental autoimmune encephalomyelitis. *Acta Neuropathol.* **118**, 219–233 (2009).
27. M. J. Carson, Microglia as liaisons between the immune and central nervous systems: Functional implications for multiple sclerosis. *Glia* **40**, 218–231 (2002).
28. U. K. Hanisch, H. Kettenmann, Microglia: Active sensor and versatile effector cells in the normal and pathologic brain. *Nat. Neurosci.* **10**, 1387–1394 (2007).
29. R. Milner *et al.*, Increased expression of fibronectin and the $\alpha 5 \beta 1$ integrin in angiogenic cerebral blood vessels of mice subject to hypobaric hypoxia. *Mol. Cell. Neurosci.* **38**, 43–52 (2008).
30. M. L. Bennett *et al.*, New tools for studying microglia in the mouse and human CNS. *Proc. Natl. Acad. Sci. U.S.A.* **113**, E1738–E1746 (2016).
31. N. N. Dagher *et al.*, Colony-stimulating factor 1 receptor inhibition prevents microglial plaque association and improves cognition in 3xTg-AD mice. *J. Neuroinflammation* **12**, 139 (2015).
32. M. R. P. Elmore *et al.*, Colony-stimulating factor 1 receptor signaling is necessary for microglia viability, unmasking a microglia progenitor cell in the adult brain. *Neuron* **82**, 380–397 (2014).
33. M. C. Papadopoulos, A. S. Verkman, Aquaporin-4 and brain edema. *Pediatr. Nephrol.* **22**, 778–784 (2007).
34. B. Engelhardt, F. K. Conley, E. C. Butcher, Cell adhesion molecules on vessels during inflammation in the mouse central nervous system. *J. Neuroimmunol.* **51**, 199–208 (1994).
35. D. L. Sparks, Y. M. Kuo, A. Roher, T. Martin, R. J. Lukas, Alterations of Alzheimer's disease in the cholesterol-fed rabbit, including vascular inflammation. Preliminary observations. *Ann. N. Y. Acad. Sci.* **903**, 335–344 (2000).
36. R. A. Adams *et al.*, The fibrin-derived gamma377-395 peptide inhibits microglia activation and suppresses relapsing paralysis in central nervous system autoimmune disease. *J. Exp. Med.* **204**, 571–582 (2007).
37. O. Hassler, Blood supply to human spinal cord. A microangiographic study. *Arch. Neurol.* **15**, 302–307 (1966).
38. I. M. Turnbull, A. Brieg, O. Hassler, Blood supply of cervical spinal cord in man. A microangiographic cadaver study. *J. Neurosurg.* **24**, 951–965 (1966).
39. V. Jolivel *et al.*, Perivascular microglia promote blood vessel disintegration in the ischemic penumbra. *Acta Neuropathol.* **129**, 279–295 (2015).
40. N. Lou *et al.*, Purinergic receptor P2RY12-dependent microglial closure of the injured blood-brain barrier. *Proc. Natl. Acad. Sci. U.S.A.* **113**, 1074–1079 (2016).
41. S. Taylor *et al.*, Suppressing interferon- γ stimulates microglial responses and repair of microbleeds in the diabetic brain. *J. Neurosci.* **38**, 8707–8722 (2018).
42. P. Bandopadhyay, W. Selvamurthy, Suggested predictive indices for high altitude pulmonary oedema. *J. Assoc. Physicians India* **48**, 290–294 (2000).
43. A. P. Lee, L. G. Yamamoto, N. L. Relles, Commercial airline travel decreases oxygen saturation in children. *Pediatr. Emerg. Care* **18**, 78–80 (2002).
44. I. Luccarini *et al.*, Combined treatment with atorvastatin and minocycline suppresses severity of EAE. *Exp. Neurol.* **211**, 214–226 (2008).
45. R. Milner, I. L. Campbell, Developmental regulation of $\beta 1$ integrins during angiogenesis in the central nervous system. *Mol. Cell. Neurosci.* **20**, 616–626 (2002).